Naval Research Laboratory
Washington, DC 20375-5320

NRL/5320/MR—2024/2

Front-End IMD in Receive Arrays: How Beamforming Sums Combine ADC Spurs

J. O. COLEMAN (RETIRED)

Advanced Radar Systems Branch
Radar Division

March 7, 2024

REPORT DOCUMENTATION PAGE

PLEASE DO NOT RETURN YOUR FORM TO THE ABOVE ORGANIZATION

1. REPORT DATE	2. REPORT TYPE	3. DATES COVERED	
		START DATE	END DATE
07-03-2024	NRL Memorandum Report	October 1, 2012	September 30, 2014

4. TITLE AND SUBTITLE
Front-End IMD in Receive Arrays: How Beamforming Sums Combine ADC Spurs

5a. CONTRACT NUMBER	5b. GRANT NUMBER	5c. PROGRAM ELEMENT NUMBER
5d. PROJECT NUMBER	**5e. TASK NUMBER**	**5f. WORK UNIT NUMBER**
		1E88

6. AUTHOR(S)
J. O. Coleman*

7. PERFORMING ORGANIZATION / AFFILIATION NAME(S) AND ADDRESS(ES)
Naval Research Laboratory
4555 Overlook Ave SW
Washington, DC 20375-5320

8. PERFORMING ORGANIZATION REPORT NUMBER
NRL/5320/MR—2024/2

9. SPONSORING / MONITORING AGENCY NAME(S) AND ADDRESS(ES)	10. SPONSOR / MONITOR'S ACRONYM(S) NUMBER	11. SPONSOR / MONITOR'S REPORT NUMBER(S)
Office of Naval Research One Liberty Center 875 N. Randolph Street, Suite 1425 Arlington, VA 22203-1995	ONR	

12. DISTRIBUTION / AVAILABILITY STATEMENT
DISTRIBUTION STATEMENT A: Approved for public release; distribution is unlimited.

13. SUPPLEMENTAL NOTES
*Retired

14. ABSTRACT
Here the effects of placing an identical memoryless nonlinearity behind every element of an active receive array are first reviewed, following which several recently proposed ideas for mitigating nonlinear distortion in all-digital arrays are briefly examined. Examples assume an RF-sampled S-band radar receiver, even though the concepts apply to IF-sampled systems as well. A chirp waveform with a substantial time-bandwidth product is assumed in places as well. A nonlinearity prior to the RF filter, presumably in a low-noise preamp, is considered briefly, but the focus is on distortion introduced by the ADC that presumably follows the RF filter.

15. SUBJECT TERMS

16. SECURITY CLASSIFICATION OF:			17. LIMITATION OF ABSTRACT	18. NUMBER OF PAGES
a. REPORT	b. ABSTRACT	c. THIS PAGE		
U	U	U	SAR	27

19a. NAME OF RESPONSIBLE PERSON	19b. PHONE NUMBER *(Include area code)*
Greg Tavik	(202) 404-1945

This page intentionally left blank.

CONTENTS

This page intentionally left blank.

FRONT-END IMD IN RECEIVE ARRAYS: HOW BEAMFORMING SUMS COMBINE ADC SPURS

1. INTRODUCTION

The primary purpose of this report is to review the effects of placing an identical memoryless nonlinearity behind every element of an active receive array. It is intended as background information for those considering possible approaches to remediation.

While not its primary focus, this report does indeed conclude, in Section 5, with a brief examination of several recently proposed ideas for mitigating nonlinear distortion specifically in all-digital arrays. Along the way, however, other approaches specific to receivers or radar systems but not to arrays—simple filtering, pulse compression, etc—are at least superficially examined, and some of those turn out to be quite useful. The work of Lauritzen [1], discussed further below, is worth a look as well, as he presents some approaches specific not to radar or antenna arrays but to parallel analog-to-digital converters (ADCs) in general. Some of his approaches are specific to bandpass sampling as would be used in digital receivers. As we will see though, no mitigation approach can improve matters for all spurious terms created by these nonlinearities.

This report's many examples assume an S-band radar receiver using bandpass sampling at RF, even though the concepts apply to IF sampling as well. A chirp waveform with a substantial time-bandwidth product is assumed in places. A nonlinearity prior to the RF filter, presumably in a low-noise preamp, is considered briefly, but the focus is on distortion introduced by the ADC that presumably follows the RF filter.

This report is not really a research paper, as most of its material is widely known to those working in the field. Though it is surely intended for those who have not worked before with nonlinear terms in digital receive arrays, it is not quite a real tutorial either, because it simply is not that well thought out. Instead it's a sort of informal stand-in for that tutorial, something that will have to do in the absence of a mandate, the funding, or the time to develop an actual tutorial. In truth it's the report of my own early learning curve as I began sorting through questions of how nonlinear ADC conversion products correlate across time and space. This is how I discovered where the nonlinear terms end up in frequency and beamspace and how they fare in a radar receiver's pulse-compression filtering. In spite of its informality, it is checked over well enough that I'm reasonably confident of its correctness.

1.1 Harmonics or Two-Tone Tests?

First, some minor observations on how nonlinear performance is specified.

Why when thinking about nonlinearity do RF designers focus on two-tone IMD (intermodulation distortion) tests, while ADC makers largely concern themselves exclusively with harmonics, speaking of total harmonic distortion or dB suppression levels for single-tone-test spurs?

Manuscript approved March 6, 2024.

All RF designers understand that since RF systems mostly remove harmonics fairly cleanly, two-tone testing is required so that they can see in-band nonlinear products. This is particularly true of the narrowband systems that dominated the field until fairly recently.

In ADCs, a harmonics-only view is consistent with the single-tone test paradigm that has always dominated testing. In that single-tone world, nonlinear distortion, for example through imperfect positioning of quantization levels, reveals itself as spurious tones arising as aliased harmonics. It's only modestly tongue-in-cheek to observe that this most likely provided sufficient measurement excitement that there was little reason, from the ADC-designer point of view, to move towards a two-tone paradigm until relatively recently, when RF designers began to use ADCs to do bandpass conversion. Tradition is a powerful force though, and harmonic spurs still dominate ADC spec sheets. Further, nonlinear distortion in audio engineering has long been summarized by a single number, total harmonic distortion, and to some extent, it appears that the ADC community simply picked up this outlook.

The single-tone mentality is so pervasive in the ADC field that the existence of, say, a third-order distortion term is apt to be disguised in the spec sheet as information on aliased third-harmonic spurs or even buried in numbers for spur-free dynamic range (SFDR). But the phenomenon underlying an aliased third harmonic is generally simple odd-order memoryless distortion. Of course this distortion creates IMD as well, and IMD behavior is apt to be just as important as harmonic behavior in the big picture. Further, the use of SFDR to characterize nonlinear behavior unfortunately suggests that these aliased-harmonic (and IMD) spurs remain a constant number of dB below the desired signal. Of course that's not true.

Sometimes too much weight is put on SFDR numbers by receiver designers who forget that if the third-order term in the ADC is swamped by the third-order term in the low-noise preamp or mixer, then the ADC SFDR may be more or less irrelevant.

1.2 A Menagerie of Nonlinear Terms

Lauritzen's first-rate dissertation work [1] examines the origin of and the correlation between harmonics generated by multiple high-performance ADCs of the same type driven by a common sinusoidal signal. He does talk of harmonics, not of IMD, but still his taxonomy of error sources provides useful orientation.

Taxonomy first. Lauritzen divides nonlinear ADC distortion into quantizer distortion and sampler distortion, the latter being distortion created in the sample/hold process. He then subdivides sampler distortion into continuous-time sampler distortion, time-varying sampler distortion, and, using not quite the same name as the broad category, sampling distortion. His breakdown of sampler-distortion types this way according to the underlying physical mechanism follows Yu et al. [2].

One of these four types of nonlinear ADC distortion, quantizer distortion, is theoretically memoryless, and Lauritzen's measured results are consistent with this. However, from his Fig. 3.27, which presents the error term computed from the instantaneous input-output curve of an ADC, the quantizer transfer function, for 16 nominally identical high-performance ADCs, we can see that while there is a significant common component to those transfer functions, that common component is not the whole story. There are also significant components of the quantizer error that differ from one device to another. Indeed, Lauritzen saw that when ADCs were driven by a common sinusoidal signal, harmonics due to quantizer error were only partially correlated.

Sampler distortion, however, appeared to be essentially identical from device to device, and harmonics from that source were consistently well correlated. None of the three types of sampler distortion Lauritzen discusses is memoryless, however, a conclusion supported both by his high-level description of physical distortion mechanisms and by his measured data.

Ultimately Lauritzen asserts that both quantizer distortion and sampler distortion are typically significant but also that either can dominate in a particular case. The circuit mechanisms underlying these distortion types suggest that sampler distortion should be much less severe at lower clock rates, when the ADC is not so much pushed speedwise. Indeed, the analytic models taken from Yu et al. show substantial dependence on the drive frequency, with some harmonics varying as f^2 and others varying, for the kth harmonic, as $f^{2(k-1)}$. (The models from Yu et al. do not consider the useful cancellation of even-order distortion terms commonly obtained in ADC front ends by using differential sampling, so this k dependence should not be taken as anything like a complete picture.)

1.3 Focus on Correlated, Memoryless Nonlinear Errors

The present report works with memoryless nonlinearities that are identical from one array element to another. This fits the correlated part of quantizer distortion. The other part of quantizer distortion is memoryless but uncorrelated, so for that part some of the effects discussed here will manifest, but some, particularly beamspace effects, will not. Sampler distortion is correlated, but because of the memory it exhibits, beamspace properties of the nonlinear signal terms it creates may or may not follow the scheme outlined in this report. One should be cautious here.

Overall then, this report focuses on nonlinear terms that are likely significant but may or may not be dominant in a given case, and for the other terms there may be some unpredictable partial relevance of the ideas here. In particular, the nonlinearity-mitigation approaches in Section 5, because they deal for the most part with spatial or beamspace phenomena, may well be irrelevant to sampler distortion. Lauritzen does discuss some mitigation approaches for harmonics created in parallel ADC banks in general, and these are worth a look as candidates for mitigating the effects of sampler distortion and noncorrelated quantizer distortion.

1.4 Begin with Third-Order Terms

At the elements of an all-digital receive array, both the RF front ends and the front-end electronics in the ADCs will exhibit IMD that as a first approximation anyway is consistent with a memoryless nonlinearity. Using differential signals everywhere in the RF/ADC chain generally reduces much even-order distortion to irrelevant levels, so the dominant issue might seem to be odd-order distortion. And it is indeed so for amplifiers. But if you begin with the input-output characteristic of an ADC, the quantizer transfer function, and subtract the ideal input-output characteristic to keep only the distortion, you are not likely to end up with an odd function. ADC distortion need not be symmetric above and below the zero point as with a well-balanced differential amplifier. So even-order terms matter, even if they perhaps matter less than odd-order terms.

That said, here the focus at first will be on the third-order term because (1) for preamp nonlinearity it is apt to be dominant, (2) because it is the lowest-order distortion that creates in-band IMD terms, and (3) because it illustrates the approach to analysis and understanding that can be applied to distortion of any order. Eventually, both second-order terms and higher-order nonlinear terms will be brought into the picture.

1.5 The Key Questions

The real question addressed here using a correlated, memoryless model of nonlinear distortion is this: how do harmonics and IMD behave in the array setting? How do phase-steering weights, an aperture taper, and the beamforming sum affect it? Finally, can the mitigation techniques discussed in the literature [3, 4, 1, 5] (and elsewhere) for nonlinear errors in antenna and ADC arrays provide relief? Of particular interest here: can inserting nominally canceling phase shifters or delays before and after key nonlinearities potentially mitigate any part the problem?

2. AN ASSUMED RECEIVER STRUCTURE

It turns out that the fate of nonlinear terms depends heavily on receiver structure, so no one analysis can cover all cases. Let us assume the digital-receiver structure of Fig. 1, which is a slightly simplified variant of the type of architecture explored in detail in [6]. This structure has features that will illustrate important nonlinear-response issues not typically considered by designers.

The frequency-domain sketches in Fig. 1 follow the conventions of [7] and use $\times$ to filter with frequency responses and $\star$ to sample or decimate by convolving with impulses. For efficiency, implementation would order the steps as shown in (a), using the individual-stage input and output sample rates marked with the $\vee$ ticks. (Further, filtering and subsequent decimation would always be combined for efficiency.) But the easiest way to analyze the system's operation is to first commute the sampling and first decimation steps downward, past the filters. The commuting operations do not affect the filter frequency responses, because every spectral impulse moved lies at a multiple of the period of every frequency response passed in the move. The commutation groups the $\times$ steps and the $\star$ steps so that they can be combined for simplification. Combining the digital filters and combining sampling and both decimations yields the simple system of (b). The desired behavior is easiest to understand if the two filters of (b) are combined as well, but that combination is left to the imagination for the sake of discussion of nonlinear terms below. The two filters together become an analytic (positive frequencies only) bandpass filter that passes the 3.1 to 3.5 GHz signal band with narrow transition regions, of width equal to 3.3 GHz $/7 - 400$ MHz ≈ 71.4 MHz, above and below that passband. The output of this equivalent analytic filter is a complex signal that is then sampled at 3.3 GHz$/7$ to create an IQ signal with signal band between ± 200 MHz.

The receiver of Fig. 1 can be taken to be a wideband digital front end only, in that the expectation is that its wideband output signal would then be—this is not shown—further shifted in frequency by a complex exponential, further narrowband filtered, and further decimated to an even lower sample rate, finally retaining a signal band extending over an interval of width somewhere in the range of 1 MHz to 100 MHz. Final filtering matched to or designed to operate with the transmitted pulse would follow.

The nonlinear vulnerability flagged in Fig. 1 is discussed below after some preliminary analysis of nonlinear terms.

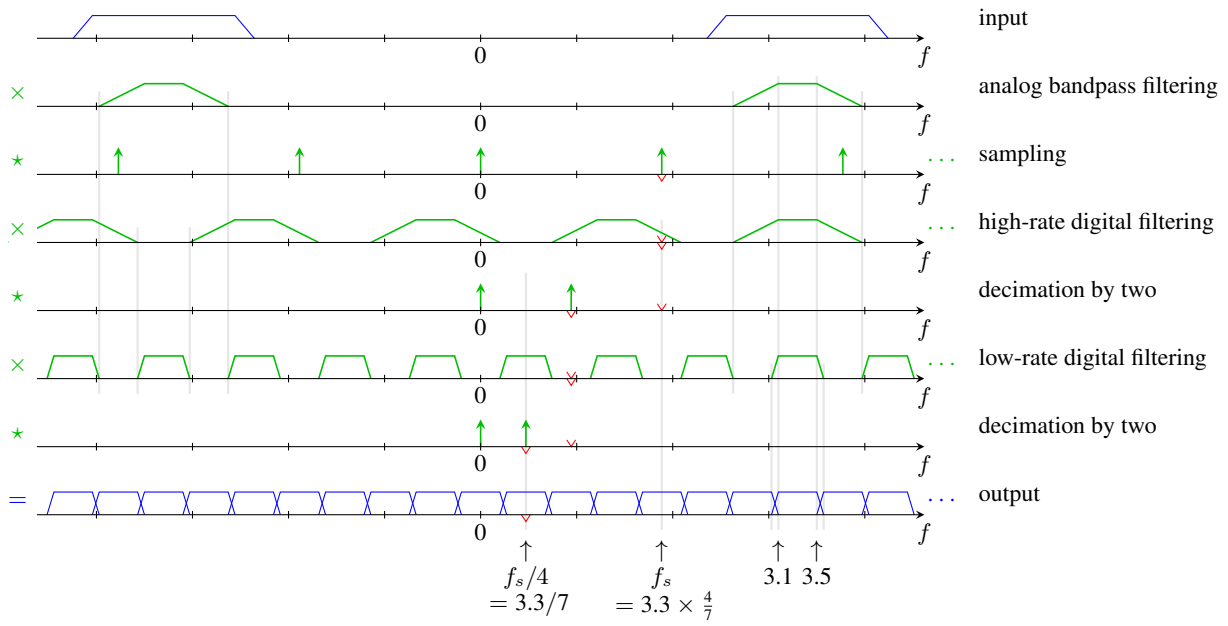

(a) System as implemented.

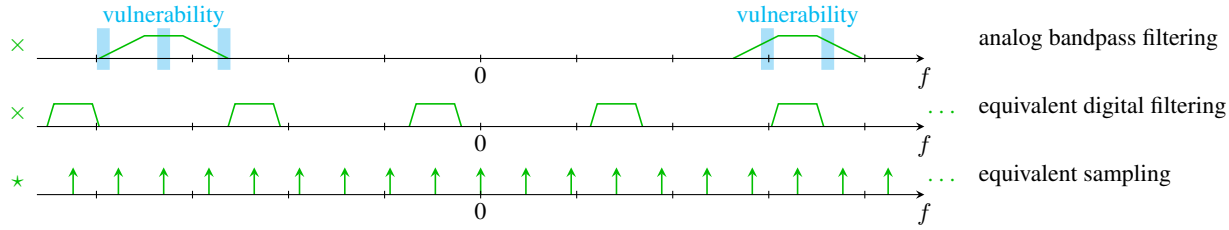

(b) Equivalent system for analysis.

Fig. 1 — S-band IQ receiver using RF sampling in the fourth Nyquist zone. The third-harmonic vulnerability shown is detailed in Fig. 2(a).

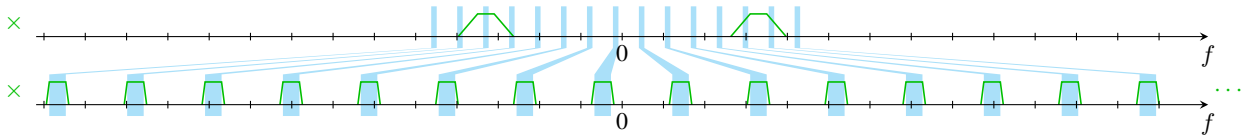

(a) Third-harmonic vulnerability zones.

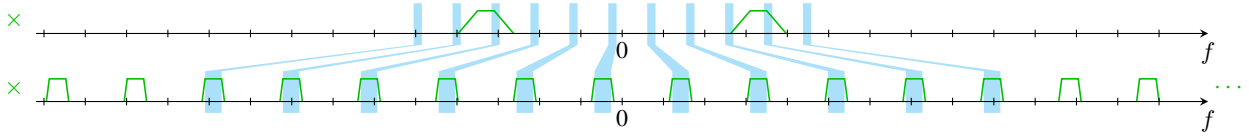

(b) Second-harmonic vulnerability zones.

Fig. 2 — A signal at the analog-filter output lies in an Nth-harmonic vulnerability zone of the Fig. 1 digital receiver if its Nth harmonic falls into a passband of that system's equivalent digital filter. Those two filters are here shown on a compressed frequency scale.

3. THE THIRD-ORDER TERMS CREATED BY TWO SOURCES

A far-field plane-wave incident on the array at frequency ω and with wavenumber vector $\mathbf{k}$ creates an element-output signal of the form

$$A\,\mathrm{e}^{\,j(\omega t-\mathbf{k}\cdot\mathbf{x})}+A^*\mathrm{e}^{-j(\omega t-\mathbf{k}\cdot\mathbf{x})},$$

where complex amplitude A depends on source strength and phase and on the amplitude and phase of the embedded element pattern at frequency ω and in the DOA associated with $\mathbf{k}$. Suppose two such signals are incident and that the element output is passed through a third-order nonlinearity. Some shorthand will help us. Let

$$\begin{aligned} a &= A\,\mathrm{e}^{\,j(\omega_a t-\mathbf{k}_a\cdot\mathbf{x})},\\ b &= B\,\mathrm{e}^{\,j(\omega_b t-\mathbf{k}_b\cdot\mathbf{x})} \end{aligned} \tag{1}$$

so that the two signals are $a+a^*$ and $b+b^*$. The resultant distortion term is proportional to

$$\big((a+a^*)+(b+b^*)\big)^3=(a+a^*)^3+3(a+a^*)^2(b+b^*)+3(a+a^*)(b+b^*)^2+(b+b^*)^3.$$

Expanding this out will create $4^3=64$ terms. Let's first look at those with positive frequencies, remembering that the conjugate of each is an associated negative-frequency term. A term has a positive frequency if it has fewer conjugated factors than not. The 32 such terms are

$$\begin{aligned} a^3+3a^2a^*+3(a^2+2aa^*)b+3a^2b^*+3a(b^2+2bb^*)+3a^*b^2+b^3+3b^2b^* & \\ = \;& a^3+b^3 && \text{harmonics}\\ &+3(|a|^2+2|b|^2)a+3(|b|^2+2|a|^2)b && \text{compression}\\ &+3a^2b+3ab^2 && \text{harmonic IMD}\\ &+3a^2b^*+3a^*b^2 && \text{classic IMD.} \end{aligned} \tag{2}$$

The terms can be categorized as shown and each category considered separately.

We'll work with a single element, but given identical hardware behind each element, the same signals appear in each with only the element location $\mathbf{x}$ changed. This will make every nonlinear term that appears look to the system like an incident plane wave. (It is possible for these nonlinear terms to appear in invisible space, but this will not be typical.) Such a term will loom large at the array output if the beam points in its direction, exactly as if it were an actual signal. However, in an all-digital array the nonlinear interaction creating these terms occurs before beamforming, so actual sources well outside the beam—even far from it—or outside the band can produce nonlinear terms that appear to be at beam center and band center.

3.1 The Compression Terms

The compression terms in (2) are the least interesting, because the complex magnitudes leave each term with just one of the original complex exponentials. That means each of these terms appears at the frequency and from the direction of one of the two original signals, simply changing the magnitude of the signal in a way that is nonlinear in the original amplitudes. The third-order term in an RF amplifier generally has

a negative sign, so the net effect is the compression we see at the top of the original-signal curves in a third-order intercept chart. In an ADC we do not know the sign of the third-order term, so the net effect can actually be enhancement rather than compression. And while it concerns us little here, it is interesting to note in passing that the amplitude signal a's compression term depends on the amplitude of signal b. Each signal can compress (or enhance) the other.

Each conjugate of such a compression term has $\omega < 0$ and so will be filtered out by the receiver's analytic bandpass filtering, making it irrelevant.

3.2 The Harmonic Terms

The harmonic terms are the simplest to understand, but careful analysis reveals them to be less important here than engineering intuition might suggest. To begin, a plane wave at frequency ω, wavenumber vector $\mathbf{k}$, and complex amplitude A has third-harmonic terms

$$a^3 = A^3 \, \mathrm{e}^{\,j(3\omega t - 3\mathbf{k}\cdot\mathbf{x})},$$
$$a^{*3} = A^{3*} \, \mathrm{e}^{-j(3\omega t - 3\mathbf{k}\cdot\mathbf{x})}$$

that appear to be from a plane wave of frequency 3ω, wavenumber vector $3\mathbf{k}$, and complex amplitude A^3. These tripled plane-wave parameters strongly affect how these terms are processed by a particular receiver structure.

Let us consider frequency first using the Fig. 1 receiver structure. There are three cases.

Preamp a^3 terms.

In Fig. 1(b) the passband of the analytic bandpass filter—the two filters shown taken together—comprises frequencies within 200 MHz of its 3.3 GHz band center. A term a^3 that originates in a preamp preceding the analog filter therefore has a frequency 3ω that falls into the filter's passband only if the signal frequency is within $200/3 \approx 67$ MHz of $3.3/3 = 1.1$ GHz. There is likely to be some rudimentary filtering before the preamp, even if only that inherent in the element design, that precludes the possibility of such terms being an issue. Since third-harmonic amplitudes go as the cube of the original amplitudes, the latter filtering need not be severe in order to be effective.

Preamp a^{*3} terms.

These terms have negative frequencies and do not survive analytic filtering.

ADC a^3 terms.

Signal a must survive the positive-frequency passband of the analog filter in order to cause harmonic term a^3 to be generated in the ADC that follows it. For that harmonic term to then survive the equivalent digital filter in Fig. 1(b) and ultimately end up in the receiver output's passband, 3ω must fall into one of that equivalent digital filter's passbands. For a term originating in this harmonic to appear at the receiver output, both of these survival requirements must be met, so ω itself must fall into one of two positive-frequency vulnerability zones in the analog filter's transition bands. See Fig. 2(a) for clarification.

ADC a^{*3} terms.

In order for signal a to survive the negative-frequency passband of the analog filter and then for 3ω to fall into a passband of the equivalent digital filter in Fig. 1(b), ω itself must fall into one of three negative-frequency vulnerability zones. One of these is in the center of the negative-frequency passband of the analog filter. The other two are at the outer edges of its transition band (which invites a slight respecification of that transition band).

3.2.1 Further Filtering

If a harmonic term survives the filtering in the Fig. 1 receiver, it presumably encounters further selectivity that reduces the net passband width from 400 MHz to perhaps something between 1 MHz to 100 MHz. This effectively shrinks the width of each vulnerability zone shown down to a subset with width in the range of $1/3$ MHz to $100/3$ MHz. In this discussion we do not control ω, as it is not the frequency to which the receiver or radar is tuned but is the frequency of an unknown interferer. Still, vulnerability here is very limited, particularly for narrowband modes. That residual vulnerability is further reduced by the harmonic's mismatch to the radar pulse. A quick computational experiment (courtesy D. Scholnik, NRL) shows that a chirp waveform with a time-bandwidth product of 100 gains roughly 20 dB in matched filtering relative to a mid-band CW tone.

Returning Radar Pulses.

Can third harmonics of returning radar pulses be an issue? The positive-frequency vulnerability zones in Fig. 1(b) are entirely out of band, so only out-of-band signals can produce in-band third harmonics. It follows that returning radar pulses, which are in-band by definition, cannot produce a^3 harmonics at matching receiver-output frequencies.

There is an in-band negative-frequency vulnerability zone in Fig. 1(b), and there is one signal frequency, precisely at the center of the band, which will result in the desired signal a and its a^{*3} term appearing at the same receiver output frequency, at DC in fact. Shifting a above that midband frequency by Δf will shift signal and third harmonic at the receiver output by Δf and $-3\Delta f$ respectively, so deviation from the band center quickly reduces the risk. More importantly, the same line of argument implies that a received band-center upchirp at chirp rate $\Delta f/\text{s}$ has a harmonic that is a downchirp at rate $3\Delta f/\text{s}$, so pulse compression will suppress this term significantly. For a chirp with a time-bandwidth product of 100, this suppression appears to be on the order of 26 dB.

3.2.2 How it Differs for Other Harmonics

Only the second harmonic is considered in detail. Analysis for others proceeds along similar lines.

Fig. 2(b) repeats the vulnerability-zone analysis for second harmonics. There are vulnerability zones only at the band edges. Filtering not shown that follows the Fig. 1 system again reduces their effective width, here to something in the range of $1/2$ MHz to $100/2$ MHz.

Can returning radar pulses be an issue? Because the in-band portion of the positive-frequency second-harmonic vulnerability zone is in the zone's left half, associated second harmonics end up in the left half of

the band at the receiver output. There they cannot match the frequencies of the signals that caused them, as the latter were near the upper band edge.

The situation for the negative-frequency second-harmonic terms is less convenient. Signal term a has original frequency $\omega > 0$ and at the receiver output ends up at $\omega \bmod \omega_s$. The frequency of the associated a^{*2} term is -2ω, which at the receiver output becomes $-2\omega \bmod \omega_s$. The two receiver-output frequencies are equal if and only if ω is an integral multiple of $\omega_s/3$. Only the fifth multiple, at about 3.143 GHz, is in-band. Even at that vulnerable frequency, however, a signal comprising an upchirp at rate $\Delta f/\mathrm{s}$ generates a second harmonic term that is a downchirp at rate $2\Delta f/\mathrm{s}$. The mismatch penalty is substantial: a chirp with a time-bandwidth product of 100 has roughly a 23 dB advantage over the wrong-way double-rate chirp in a matched filter.

3.2.3 Where Do Harmonics Appear Spatially?

As we just saw, it is primarily the filtering that determines how much harmonic content will survive to cause interference. A spatial analysis will show where such residual interference will appear to be in beamspace.

Consider the beamspace of Fig. 3, which can be assumed drawn on the array plane itself. A black dot marks the origin, and periodic hexagons represent periods of the array factor, assuming a planar array on an equilateral triangular grid and with the hexagon size determined by element spacing. Suppose the wavenumber vector $\mathbf{k}$ of a positive-frequency incident plane wave projects onto beamspace at the larger dot, on the ray an hour hand would point to at 10:30 or so. The system interprets this location as a direction according to where it falls in a visible space. That visible space has radius proportional to frequency, and a narrowband array is typically designed with element spacing and frequency related so that at the top of the tuning range, the visible space is inscribed in the hexagon containing the origin.

The third-harmonic term appears at a different location in beamspace, at $3\mathbf{k}$ as marked with the smaller dot on that same ray, as well as at a different frequency. For the other example, on the ray near 7:30, the $3\mathbf{k}$ position falls into a different hexagonal array-factor period. All the outer hexagons are spatially aliased onto the center one, so the harmonic is aliased to the position so labeled, on the parallel aliased ray entering the center hexagon near the 2:30 hour-hand position.

Figure 4 shows many harmonics of each of two sources.

In Figs. 3 and 4 only positive harmonics are shown. The receiver is explicitly designed to filter out the "-1th harmonic", so there is never a dot at $-\mathbf{k}$. But the a^{*3} term may survive the filtering, so to be fully proper, the drawings should also show a dot at $-3\mathbf{k}$ for each source signal. These are left to the imagination for now.

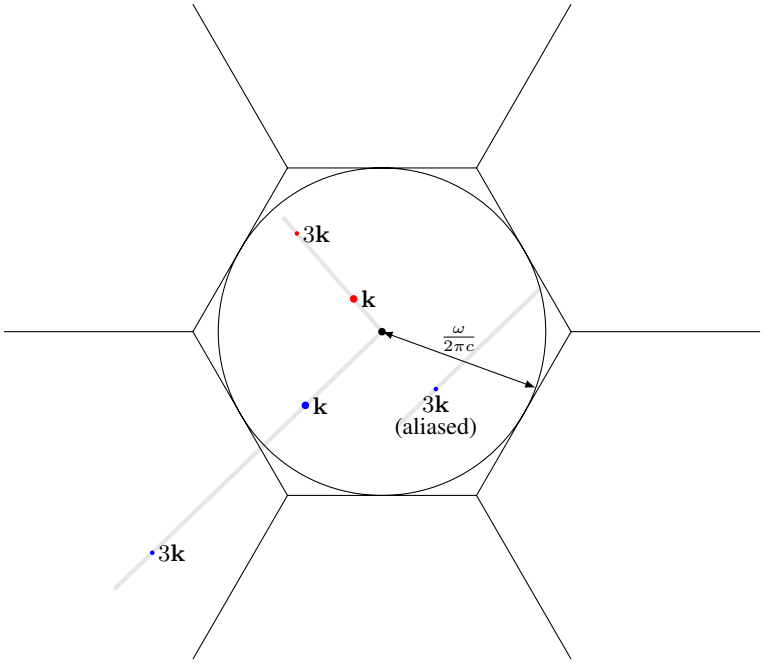

Fig. 3 — Third-harmonic geometry.

3.2.4 Summary for Harmonics

The important points:

1. Harmonics of transmitted radar signals are an issue at very few, very specific operating frequencies (the number of such frequencies will generally increase for higher-order harmonics) or, more precisely, close enough to those specific frequencies for signal and harmonic to overlap spectrally to a significant degree.
2. Even at those frequencies, if the original signal is a chirp, the Nth harmonic will be a chirp at $\pm N\times$ the original frequency slope, so pulse-compression mismatch will contribute significant harmonic suppression.
3. Harmonics of other incident signals are an issue only if those signals are in particular frequency subbands determined by receiver structure. Even In those bands, pulse compression generally provides useful attenuation.
4. A harmonic appears to be coming from a direction that generally differs from the actual direction of the signal that creates it. Much of the time it will fall in array sidelobes and so be further attenuated. If the volume is being searched, however, the beam will hit it eventually if it falls within the search volume.

Weak harmonic-based phantom ground or sea clutter may appear at positions where no actual land or sea clutter appears, at positions that are beyond the clutter horizon.

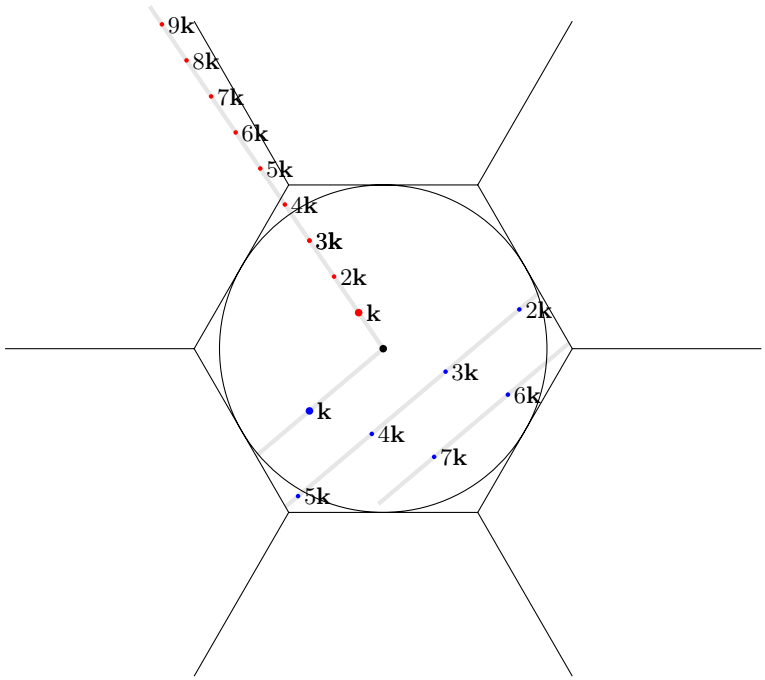

Fig. 4 — Fundamental through 9th harmonic for one signal and through 7th harmonic for another, with the spatial aliasing of the latter shown explicitly. In each case one harmonic just happens to fall in the invisible region where the steered beam will never meet up with it.

3.3 The Harmonic-IMD Terms

Signals a and b of (1) create harmonic-IMD terms

$$\begin{aligned} 3a^2\ b &= 3A_a^2\ A_b\, \mathrm{e}^{j((2\omega_a+\omega_b)t-(2\mathbf{k}_a+\mathbf{k}_b)\cdot\mathbf{x})}, \\ 3a^{*2}b^* &= 3A_a^{*2}A_b^*\, \mathrm{e}^{-j((2\omega_a+\omega_b)t-(2\mathbf{k}_a+\mathbf{k}_b)\cdot\mathbf{x})} \end{aligned}$$

at pre-aliasing frequency and wavenumber $\pm(2\omega_a+\omega_b)$ and $\pm(2\mathbf{k}_a+\mathbf{k}_b)$ respectively, where leading signs match. Swapping "a" and "b" creates two similar terms.

Negative-frequency harmonic-IMD terms from preamp distortion do not survive analytic filtering and so are irrelevant. Positive-frequency harmonic-IMD terms from preamp distortion are suppressed by any rudimentary filtering before the preamps, even that inherent in the element design, in the same way as for harmonic terms. Terms that do survive will be significantly attenuated in pulse compression, with a few extra dB of attenuation in the case in which the source terms are from the radar. The exception to the latter is one CW term and one radar pulse. In this case one of the harmonic-IMD terms is just a radar pulse and compresses perfectly.

For ADC-originated harmonic-IMD terms to matter, the source terms at both ω_a and ω_b must survive analog bandpass filtering. Positive-frequency terms must then have either

$$\frac{2\omega_a + \omega_b}{3} \qquad \text{or} \qquad \frac{\omega_a + 2\omega_b}{3} \tag{3}$$

(frequencies between those of the two source terms) fall into a positive-frequency vulnerability zone in Fig. 1(b) and, in fact, into a subset of that zone determined by the mode-dependent bandwidth reduction that follows the system shown. Negative-frequency terms must have either

$$-\frac{2\omega_a + \omega_b}{3} \qquad \text{or} \qquad -\frac{\omega_a + 2\omega_b}{3}$$

(frequencies between those of the two conjugate source terms) fall into a negative-frequency vulnerability zone in Fig. 1(b) and, in fact, into a subset of that zone determined by the mode-dependent bandwidth reduction that follows the system shown.

Returning radar pulses matter in specific contexts.

1. The worst context is, for example, when signals a and b are a CW tone and a radar pulse respectively, because then a^2b is a radar pulse at frequency $2\omega_a + \omega_b$. If the latter frequency approximates ω_b modulo ω_s, the initial sampling rate, self-interference results. This frequency setup occurs if and only if ω_a approximates an integral multiple of $\omega_s/2$. It can be seen in Fig. 1 that this happens only for specific ω_a values in the outer parts of the analog filter's positive-frequency transition bands.
2. When signals a and b are as above, $a^{*2}b^*$ is a radar pulse at frequency $-2\omega_a - \omega_b$. If the latter frequency approximates ω_b modulo ω_s, self-interference results. This occurs if and only if the average of ω_a and ω_b approximates an integral multiple of $\omega_s/4$. In Fig. 1 the integral multiple that matters lies at the band center, so a CW tone and a radar signal located symmetrically above and below this frequency will be troublesome. This situation is less severe than the one above, because here the chirp has changed direction, allowing pulse compression to help with suppression.
3. If the radar operating frequency is at (near) the specific frequencies identified in the Section 3.2.1 discussion on returned-pulse harmonics and two strong scatterers appear in the same range cell at different Doppler shifts, they will create harmonic-IMD terms at (near) the same nominal frequency but with Doppler shifts interpolated between (a third of the way across) the original shifts. Here pulse compression helps as for third-harmonic terms.

If frequencies are such that a harmonic-IMD term survives, where will it appear to be in beamspace? Figure 5 shows example relationships. In each color group, the unaliased beamspace locations of the two signal terms, the two harmonic terms, and the two harmonic IMD terms are shown, along with aliased locations where appropriate. The two harmonic-IMD terms appear in beamspace between the two harmonic terms, and in fact the decibel levels of the harmonic-IMD terms are almost interpolated between the decibel levels of the two harmonic terms in the same way, at $1/3$ and $2/3$ across the gap. The word "almost" refers to the fact that the harmonic-IMD terms are stronger than this calculation suggests by an amplitude factor of 3 or some 9.54 dB. When two signals of nearly the same amplitude intermodulate in this way, their harmonic-IMD terms are stronger than their harmonic terms.

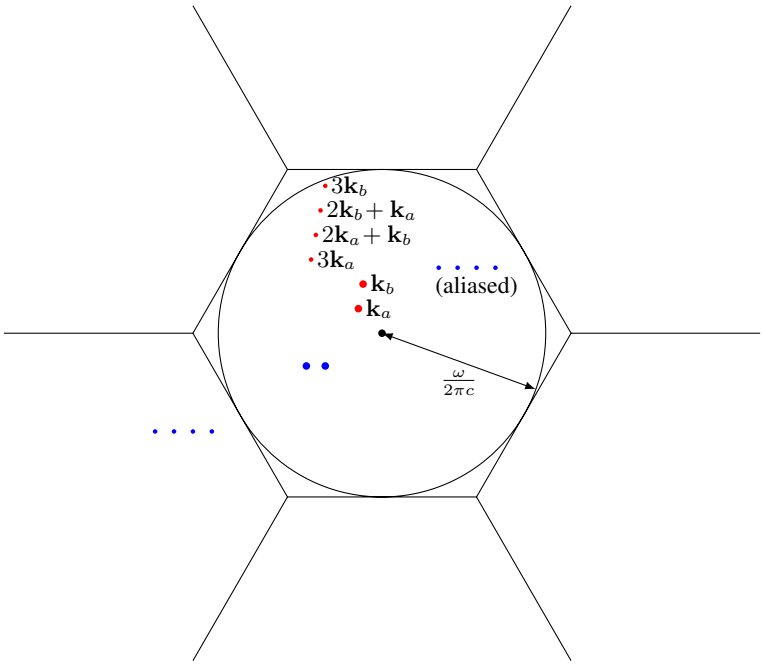

Fig. 5 — Third-harmonic and third-harmonic-IMD terms for two point-source signals.

In Fig. 5 only terms with positive temporal frequencies are shown, but negative-frequency terms may survive the filtering, so to be fully proper, each row of four dots shown should be mirrored through the origin to represent the conjugate terms with a second row of dots.

3.4 Classic IMD

The classic third-order IMD products comprise terms

$$\begin{aligned} 3a^2b^* &= 3A_a^2 A_b^* \, \mathrm{e}^{j((2\omega_a - \omega_b)t - (2\mathbf{k}_a - \mathbf{k}_b)\cdot\mathbf{x})}, \\ 3b^2\,a^* &= 3A_b^2 A_a^* \, \mathrm{e}^{j((2\omega_b - \omega_a)t - (2\mathbf{k}_b - \mathbf{k}_a)\cdot\mathbf{x})} \end{aligned}$$

which are most often at positive frequencies (the second of these occasionally isn't), and their conjugates. These are the array equivalents of the usual 3rd-order IMD terms encountered in radio engineering. The concept of the third-order intercept point applies in full.

A system with input x and outputs proportional to $x + \beta x^3$, if x is well below the compression point, has the following spectral outputs when a and b are equal-strength radar chirps, presumably strong returns, perhaps from clutter components, at different Doppler shifts. The Doppler shift is much exaggerated here for clarity.

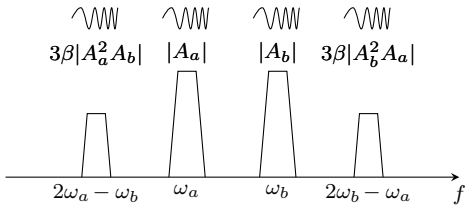

This type of IMD is potentially the most troublesome because, at least when the difference in Dopplers is small, little is lost in pulse compression. Chirps in, chirps out. Same direction. Same chirp rate (essentially).

Aside: Can the radar waveform be chosen cleverly so that the matched filter will not peak up well on these classic IMD terms? Consider signals

$$a = m(t)\,\mathrm{e}^{\,j(\omega_a t - \mathbf{k}_a\cdot\mathbf{x})}$$
$$b = m(t)\,\mathrm{e}^{\,j(\omega_b t - \mathbf{k}_b\cdot\mathbf{x})}$$

where complex function $m(t)$ represents the waveform's modulation. The a^2b^* IMD term becomes

$$m(t)\,|m(t)|^2\,\mathrm{e}^{\,j((2\omega_a-\omega_b)t-(2\mathbf{k}_a-\mathbf{k}_b)\cdot\mathbf{x})}\,.$$

Suppose $m(t)$ has finite support $\mathcal{T}$. Assuming we are in the correct Doppler bin or have Doppler shifts so small as to be irrelevant, the matched-filter output peak in response to either desired signal is $\int_{\mathcal{T}}|m(t)|^2dt$. This is waveform energy and can be taken as constant, because we want to choose the best IMD-rejection waveform with detection performance fixed. Adjusting for Doppler shift if needed, the peak response of that same matched filter to the IMD term above is $\int_{\mathcal{T}}|m(t)|^4dt$. If we let $|\mathcal{T}|$ represent the Lebesgue measure of $\mathcal{T}$, Jensen's inequality yields

$$\Big(\frac{1}{|\mathcal{T}|}\int_{\mathcal{T}}|m(t)|^2dt\Big)^2 \le \frac{1}{|\mathcal{T}|}\int_{\mathcal{T}}\big(|m(t)|^2\big)^2dt$$

or

$$\frac{1}{|\mathcal{T}|}\Big(\int_{\mathcal{T}}|m(t)|^2dt\Big)^2 \le \int_{\mathcal{T}}|m(t)|^4dt.$$

We wish to choose $m(t)$ to minimize the right side with the left side constant, so this tells us that there is a bound on how well we can do. But if we have a constant-envelope waveform so that $|m(t)| = c$ for some constant c, the inequality's left and right sides each become $c^4|\mathcal{T}|$ so that the bound is met with equality. There is no possibility of doing better by varying the envelope.

Another important scenario has a a strong CW tone interferer and b a returning radar chirp. Here a dB scale is assumed with, somewhat artificially, peak height representing time-domain amplitude in each of the four components.

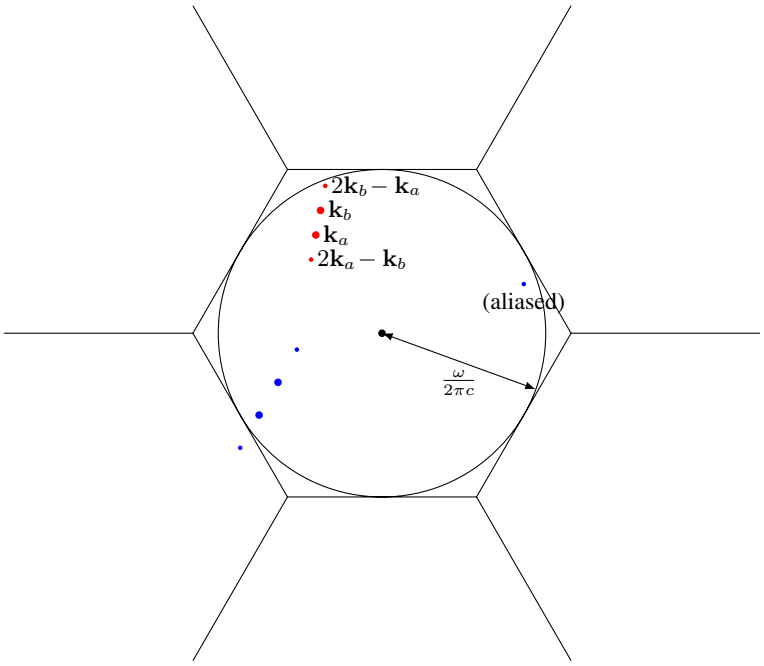

Fig. 6 — Two point-source signals and their classic third-order IMD terms.

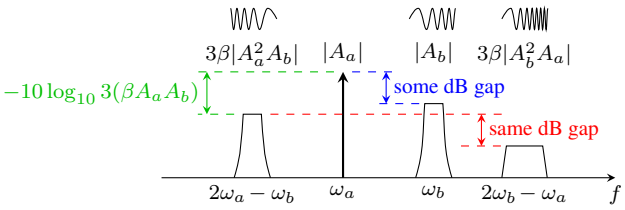

The case of most concern is the one shown, with chirp b smaller than tone a so that the larger IMD product is the opposite-direction chirp (left) on the other side of the tone from the original chirp (center right). Mismatch in the pulse-compression filter provides on the order of $10\log_{10}(BT) + 6$ dB additional suppression of this product. The same-side IMD product (right) is a double-rate chirp and gains roughly $10\log_{10}(BT) + 3$ dB additional suppression in the pulse compressor.

When the source terms are near each other spatially, these classic IMD terms appear to originate from directions very near those source terms unless spatial aliasing becomes involved. See Fig. 6. However, there is no reason to assume the intermodulating source terms are neighbors in beamspace. Strong signals from wildly different directions can intermodulate.

4. ALL THE POWER-LAW TERMS TAKEN TOGETHER

We can generalize the analysis and find the frequencies and wavenumber vectors of all the nonlinear terms created by a given power law at once. Let us work with wavenumber vectors for the sake of the

easier visualization that 2D eventually provides. In the end one can simply replace $\mathbf{k}$ with ω to get the corresponding frequencies.

If signal terms a, a^*, b, and b^* are subjected to a power-law nonlinearity of order n, the result is given by the multinomial theorem as

$$(a+b+a^*+b^*)^n = \sum_{\substack{n_1,n_2,n_3,n_4\in\{0,\ldots,n\}\\ \text{with } n_1+n_2+n_3+n_4=n}} \tbinom{n}{n_1,n_2,n_3,n_4} a^{n_1}\, b^{n_2}\, a^{*n_3}\, b^{*n_4}.$$

Let u and v denote the number of nonconjugated and conjugated factors in a term so that

$$\begin{aligned} u &= n_1 + n_2 \\ v &= n_3 + n_4. \end{aligned} \tag{4}$$

The net wavenumber vector of an individual term (before aliasing) is

$$\mathbf{k}_{\text{term}} = (n_1 - n_3)\mathbf{k}_a + (n_2 - n_4)\mathbf{k}_b, \tag{5}$$

so for the sake of a manageable mental model, suppose $\mathbf{k}_a$ and $\mathbf{k}_b$ are close in value, and suppose we are specifically interested in the terms that end up near a nonnegative multiple m of either of their wavenumber vectors. These terms are those satisfying the first of

$$\begin{aligned} u - v &= m \\ u + v &= n. \end{aligned} \tag{6}$$

The latter just re-expresses the sum's index condition $n_1 + n_2 + n_3 + n_4 = n$ using definition pair (4). We can solve (4) for n_2 and n_4 and multiply and divide (5) by m on the right to rewrite the term wavenumber vector as

$$\begin{aligned} \mathbf{k}_{\text{term}} &= \frac{n_1 - n_3}{m}\, m\mathbf{k}_a + \left(\frac{u-v}{m} - \frac{n_1 - n_3}{m}\right) m\mathbf{k}_b \\ &= \alpha\, m\mathbf{k}_a + (1-\alpha)\, m\mathbf{k}_b \end{aligned} \tag{7}$$

where the latter uses (6) and convenient definition

$$\alpha = \frac{n_1 - n_3}{m}. \tag{8}$$

Relationship (7) expresses $\mathbf{k}_{\text{term}}$ as an affine combination (linear combination with coefficients that sum to unity) of the wavenumber vectors of the mth harmonics of the two signals. An affine combination of two points lies along a straight line that passes through those points.

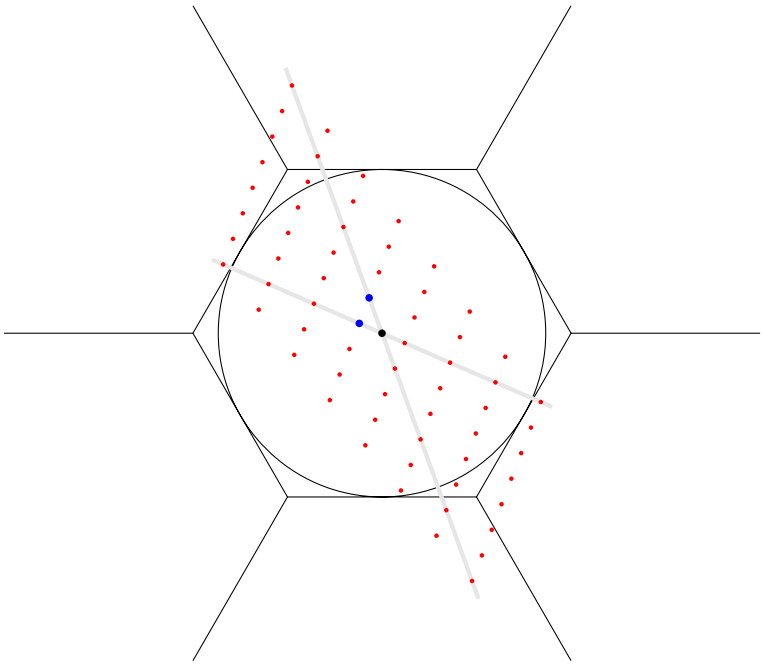

Fig. 7 — The forest of nonlinear terms created by two source signals passed through a 7th-power memoryless nonlinearity. The rays flag the pure harmonic terms.

To see how values of $\mathbf{k}_{\text{term}}$ are spaced along that line, begin with positive n and nonnegative m, either both even or both odd, and solve (6) for nonnegative integers u and v. Then definition pair (4) and conditions $0 \le n_i$ yield

$$\begin{aligned} 0 &\le n_1 \le u \\ 0 &\le n_3 \le v. \end{aligned} \tag{9}$$

Now we can pick any n_1 and n_3 that satisfy the inequalities of (9) and immediately obtain α of (8). The geometry of possible $\mathbf{k}_{\text{term}}$ values has this form.

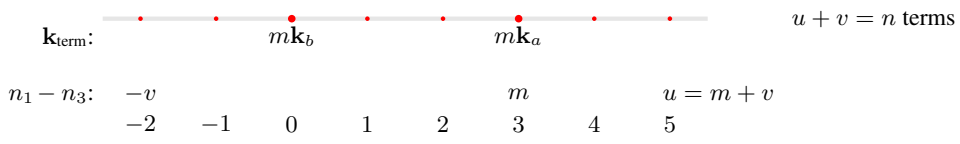

As illustrated here with $n = 7$ and $m = 3$, which imply $u = 5$ and $v = 2$, there are terms at the mth harmonics, there are $m - 1$ terms spaced evenly between them, and if $n > m$ so that $v > 0$, there are v additional terms beyond each harmonic, along the same line and at the same spacing. We have considered only the positive multiples of $\mathbf{k}_a$ and $\mathbf{k}_b$, but the conjugate terms give us the negatives of all these points as well.

The beamspace locations of the components arising from a single power term, the seventh, are shown in Fig. 7 assuming two source signals as shown. As shown in Fig. 8, lower odd powers create terms in subsets

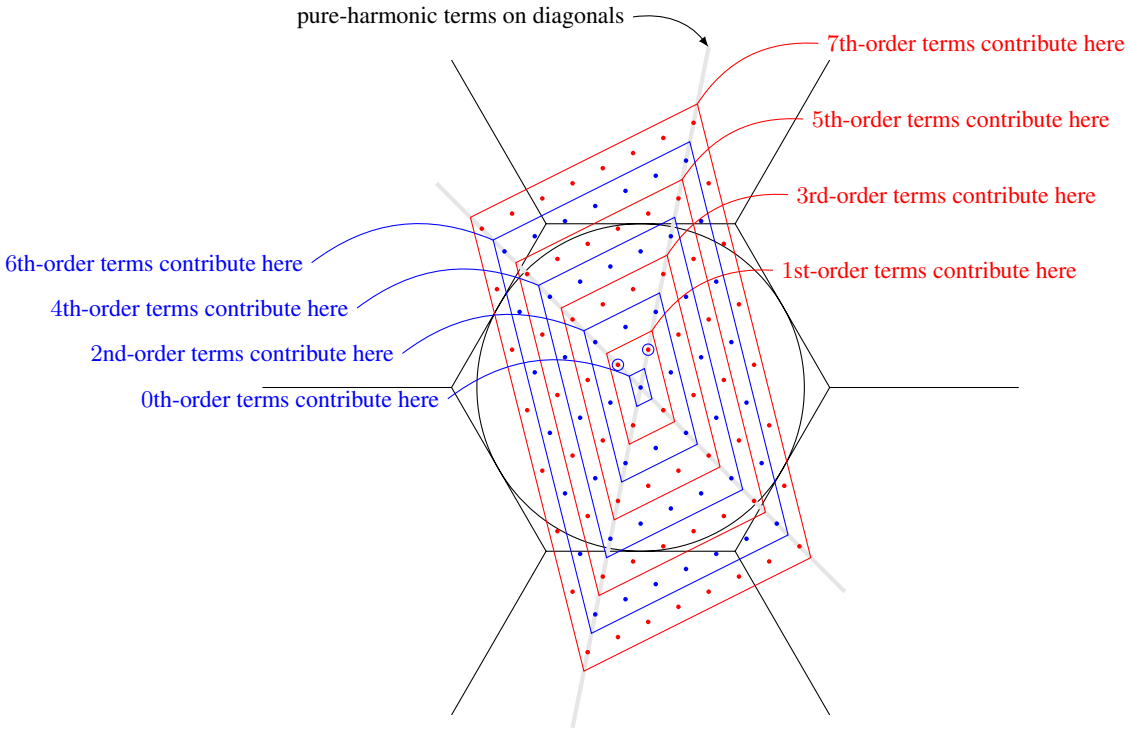

Fig. 8 — The frighteningly dense forest of nonlinear terms created by two source signals (circled) passed through a a memoryless nonlinearity $a_0+a_1x+a_1x+a_2x^2+a_3x^3+a_4x^4+a_5x^5+a_6x^6+a_7x^7$. The rays flag the pure harmonic terms, and terms arising from even-order and odd-order power terms are shown in distinct colors.

of these same locations. Even-order powers display similar subsetting, but they contribute only to affine combinations of even harmonics, including the 0th harmonic or DC.

Given power terms through the nth, the total number of spectral terms produced by two signals is $(n+1)^2+n^2$. Four of these represent the desired signals. If there are in fact some number ℓ of source terms present, considering them in pairs reveals that there are

$$\binom{\ell}{2}\left((n+1)^2+n^2\right)=\frac{\ell(\ell-1)}{2}\left(2n^2+2n-3\right)$$

spurious terms created. Of course in practice most of these will have high-power power-law sensitivity to input levels and will naturally be small. Clearly, however, even a few large source terms may be an issue if defensive measures are not taken. As we have seen, the most important defenses are (1) pulse compression with a high time-bandwidth product and (2) a digital-receiver structure with the largest possible ratio of the initial sampling rate to the final, decimated output rate. Of course corners must not be cut in the digital filters responsible for removing the spurious terms.

Pre-aliasing frequencies ω of spurious terms are calculated from ω_a and ω_b in the same way that spurious-component wavenumber vector $\mathbf{k}$ is calculated from $\mathbf{k}_a$ and $\mathbf{k}_b$. The same affine combination

is taken. The effect can be visualized by projecting the 2D array of dots in Fig. 8 onto a line. Orient the line to obtain the proper relative spacing between projected source terms.

5. ALIASED-HARMONIC MITIGATION WITH OFFSETTING PHASE SHIFTS

Lincoln Laboratory's Dan Rabideau (in [3, 4] and elsewhere) proposed shifting signal-path phase at the element at location $\mathbf{x}$ by some quantity $\phi_{\mathbf{x}}$. This scales the signal path before the nonlinearity by $\mathrm{e}^{j\phi_{\mathbf{x}}}$ and $\mathrm{e}^{-j\phi_{\mathbf{x}}}$ for positive and negative frequencies respectively. Rabideau's system then applies the factor $\mathrm{e}^{-j\phi_{\mathbf{x}}}$ digitally after the nonlinearity. Notice that a peculiar allpass filter would be required if distinct post-nonlinearity phase factors were to be applied digitally to spectral components originally found at positive and negative frequencies, because those spectral components are interlaced spectrally by the sampling process. The assumption here then is that only what was originally the positive-frequency part of the spectrum is properly phase corrected.

The idea is that our incident signals a and b are modified to become $a\,\mathrm{e}^{j\phi_{\mathbf{x}}}$ and $b\,\mathrm{e}^{j\phi_{\mathbf{x}}}$ at the point where the nonlinearity is encountered. Nonlinear terms in group m in the analysis above, those with frequencies on the order of m times those of a and b, are then generated exactly as before except that they each have an additional factor of $\mathrm{e}^{jm\phi_{\mathbf{x}}}$. The post-nonlinearity conjugate phase shift then leaves net shift $\mathrm{e}^{j(m-1)\phi_{\mathbf{x}}}$ on these nonlinear terms. The $m = 1$ group, which includes the original signals, their compression terms, and in-band IMD of all orders, are left with no net phase shift. This is why Rabideau comments that his technique does not help with in-band nonlinear terms.

The conjugate terms appear at negative frequencies just past the nonlinearity and prior to sampling, with conjugates of group m terms each having an additional factor of $\mathrm{e}^{-jm\phi_{\mathbf{x}}}$. Application of the post-nonlinearity (and post-sampling) phase shift then leaves net shift $\mathrm{e}^{-j(m+1)\phi_{\mathbf{x}}}$ on these terms. Signal-band terms, those conjugate to the $m = 1$ group, are left with net phase-shift factor $\mathrm{e}^{-j2\phi_{\mathbf{x}}}$, but these terms are generally filtered out in the receiver structure (there are exceptional cases when a and b are far apart in frequency), so the extra phase shift is irrelevant.

There are (at least) three ways to use these phase shifts that have been suggested in discussions at NRL. Let us consider them separately.

5.1 Choose Phases to Null Nonlinear Terms

We can summarize the above discussion by observing that each term with net frequency around m times the positive signal frequency (assuming source signals are close in frequency) has a net additional phase-shift factor $\mathrm{e}^{j(m-1)\phi_{\mathbf{x}}}$, where integer m can be positive or negative. The desired $m = 1$ terms are unchanged. Their $m = -1$ conjugates are filtered out. But what about the other terms?

5.1.1 Exact Nulling of an Arbitrary Nonlinear Term

For present purposes, we can assume that the original nonlinear terms are incident, with no extra phase shifts, but that instead of complex weight $w_{\mathbf{x}}$ at element position $\mathbf{x}$, the nonlinear terms see weight $w_{\mathbf{x}}\,\mathrm{e}^{j(m-1)\phi_{\mathbf{x}}}$. We must design $\phi_{\mathbf{x}}$. If we know m, we can absorb that phase factor into $w_{\mathbf{x}}$ and simply design complex weight $w_{\mathbf{x}}$ with $|w_{\mathbf{x}}|$ fixed in advance. This is a kind of phase-only (amplitudes fixed but not all the same) array-factor design problem in which array-factor nulls are desired at the wavenumber

vectors $\mathbf{k}$ at which nonlinear terms appear. Of course we do not know where to null, so the nulling approach is really no approach at all.

5.1.2 Simultaneously Minimize all Terms for Particular Harmonic

As a compromise one might give up exact nulling and have the absorbed-phase-factor optimization seek to minimize the peak array-factor value subject to fixed amplitudes on the weights. Fixing the weight amplitudes of course fixes the taper's energy and therefore the energy in the array factor as a whole, so there is no way to push the array factor down over all beamspace. It's a game of whack-a-mole.

The other problem is that we don't know m, because in reality there may be nonlinear terms for many distinct m values. An absorbed-phase-factor array factor that is whack-a-mole optimum for the second harmonic will generally be nowhere near optimum for higher-order harmonics.

5.1.3 Minimize An Own-Signal Harmonic

A variant of this scheme, one pointed out by G. Tavik and R. Mital at NRL, attempts to address only the harmonic terms arising from the radar's own returning signal. In this special case, the direction of "interferer" incidence can usually be assumed to be aligned with the array's steering direction. In principle then, one could choose the phases to simply steer the separate absorbed-phase-factor array factor that sees the harmonics so as to put an undesired harmonic term into a null. So far, so good.

5.1.4 Simultaneously Minimize Many Own-Signal Harmonics

An interesting subsidiary question arises. Is it possible to zero more than one harmonic simultaneously using this sort of scheme? Answering this question requires a much closer look.

Let us begin by quickly reviewing phase-shift steering for a 2D array of identical elements. Suppose the positive-frequency component of an incident wave has fields proportional to $\mathrm{e}^{j(\omega t-\mathbf{k}_s\cdot\mathbf{x})}$. For a planar array, the element indexed by integer column two-vector $\boldsymbol{n}$ can be assumed centered at position $\mathbf{x}=\mathbf{B}\boldsymbol{n}$, where matrix $\mathbf{B}$ characterizes the element-placement lattice. The positive-frequency component of the output of the element at that location then is proportional to $\mathrm{e}^{j(\omega t-\mathbf{k}_s\mathbf{B}\boldsymbol{n})}$ if we take wavenumber vector $\mathbf{k}_s$ to be a real row vector. To cancel the dependency on element index $\boldsymbol{n}$ so that we can sum the element outputs coherently and therefore steer a nominally boresight beam to wavenumber vector $\mathbf{k}_s$, we must multiply the positive-frequency output of element $\boldsymbol{n}$ by phase factor $\mathrm{e}^{j\mathbf{k}_s\mathbf{B}\boldsymbol{n}}$. The unsteered or boresight-aimed array factor as a function of wavenumber vector $\mathbf{k}$ has form $H(\mathbf{k}\mathbf{B})$ for some complex function $H(\,\cdot\,)$ of a real row two-vector argument [8]. It can be proved using simple Fourier-transform properties that the extra phase shifts simply translate this array factor, so when the array is steered to beamspace position $\mathbf{k}_s$, the array's response to an incident signal at beamspace position $\mathbf{k}$ is proportional to $H\big((\mathbf{k}-\mathbf{k}_s)\mathbf{B}\big)$.

Those background relationships can now be applied to our present case. Let us begin by making a sort of sequential table of various relevant quantities.

$\mathrm{e}^{j(\omega t-\mathbf{k}\mathbf{B}\boldsymbol{n})}$	normalized positive-frequency output signal from element $\boldsymbol{n}$
$\mathrm{e}^{j\mathbf{k}_e\mathbf{B}\boldsymbol{n}}$	extra phase factor imposed before ADC
$\mathrm{e}^{j(\omega t-(\mathbf{k}-\mathbf{k}_e)\mathbf{B}\boldsymbol{n})}$	signal with the extra phase factor

$\mathrm{e}^{j(m\omega t-(m\mathbf{k}-m\mathbf{k}_e)\mathbf{B}\boldsymbol{n})}$	mth-harmonic term at ADC output
$\mathrm{e}^{-j\mathbf{k}_e\mathbf{B}\boldsymbol{n}}$	conjugate phase factor imposed after ADC
$\mathrm{e}^{j(m\omega t-(m\mathbf{k}-(m-1)\mathbf{k}_e)\mathbf{B}\boldsymbol{n})}$	mth-harmonic term after conjugate phase factor applied
$m\mathbf{k}-(m-1)\mathbf{k}_e$	apparent beamspace position of nonlinear term
$H(\mathbf{kB})$	unsteered array factor for signals at wavenumber vector $\mathbf{k}$
$\mathbf{k}_s$	wavenumber vector to which array is steered
$H\big((\mathbf{k}-\mathbf{k}_s)\mathbf{B}\big)$	steered array factor
$H\big((m\mathbf{k}-(m-1)\mathbf{k}_e-\mathbf{k}_s)\mathbf{B}\big)$	net array factor seen by the mth harmonic

One key here is that $\mathbf{k}$ is at least approximately known: it matches, completely or nearly, the array's steering direction (for desired signals) $\mathbf{k}_s$. Let us therefore write $\mathbf{k}=\mathbf{k}_s+\Delta\mathbf{k}$ and suppose that $\Delta\mathbf{k}$ is small. The net array factor seen by the mth harmonic, the last item in the table, can now be rewritten as

$$H\big(((m-1)(\mathbf{k}_s-\mathbf{k}_e)+m\Delta\mathbf{k})\mathbf{B}\big). \tag{10}$$

If we want to null the mth harmonic using a null at $\mathbf{k}=\mathbf{k}_m$ in unsteered array factor $H(\mathbf{kB})$, at least in the ideal $\Delta\mathbf{k}=0$ case, the requirement then is that $(m-1)(\mathbf{k}_s-\mathbf{k}_e)=\mathbf{k}_m$ or, if we solve this for $\mathbf{k}_e$,

$$\mathbf{k}_e=\mathbf{k}_s-\frac{1}{m-1}\mathbf{k}_m. \tag{11}$$

Substituting the $m=2$ result $\mathbf{k}_e=\mathbf{k}_s-\mathbf{k}_2$ into the general relationship and solving for $\mathbf{k}_m$ establishes that for (11) to hold for some one fixed $\mathbf{k}_e$ simultaneously for all $m=2,\ldots,M$, unsteered array factor $H(\mathbf{kB})$ must have uniformly spaced nulls so that

$$\mathbf{k}_m=(m-1)\mathbf{k}_2 \tag{12}$$

for $m=2,\ldots,M$. This and the $\mathbf{k}_e=\mathbf{k}_s-\mathbf{k}_2$ design choice also allow (10), the net array factor seen by the mth harmonic, to be written as $H\big((\mathbf{k}_m+m\Delta\mathbf{k})\mathbf{B}\big)$, showing clearly the effect of nonzero $\Delta\mathbf{k}$.

One conclusion then must be that the scheme can indeed null multiple harmonics in the special case of a uniformly illuminated 1D array. The simplest version of that case involves an odd number N of elements with the center element centered on the spatial origin. Matrix $\mathbf{B}$ then has a single column, a vector extending from the origin to the center of the adjacent element, and

$$|H(\mathbf{kB})|\propto\left|\frac{\sin(N\mathbf{kB}/2)}{\sin(\mathbf{kB}/2)}\right|,$$

the numerator of which provides uniformly spaced nulls. Likewise, the scheme can work for a uniformly illuminated rectangular array, because the latter has a separable array factor with orthogonally oriented component factors that each have the form of the 1D array factor above. More generally, however, more than one harmonic cannot be simultaneously nulled, because in general the "harmonic" relationship (12) among array-factor nulls does not exist.

5.2 Steer the Harmonic Response Beam Somewhere Harmless

Wouldn't it be nice to simply use the extra phase factor in $w_{\mathbf{x}}\,\mathrm{e}^{\,j(m-1)\phi_{\mathbf{x}}}$ to steer the beam that sees the harmonics to someplace where they never appear? If there were such a place, it would be a temptation, at least if we were willing to choose a nonlinear-term group m to target. There is no such place. The harmonics can even be in the invisible region, as in the Fig. 4 examples. They never propagate in free space and are not limited by propagation physics, which is what creates the visible region. So "resistance is futile."

5.3 Random Phases

Rabideau considered choosing the phases randomly and with no correlation from one element to another. Let each $|w_{\mathbf{x}}|$ be fixed as before, but let $\mathrm{e}^{\,j\phi_{\mathbf{x}}}$ be uniformly distributed over the circle. Then $\mathrm{e}^{\,j(m-1)\phi_{\mathbf{x}}}$ is uniformly distributed over the circle as well, and $w_{\mathbf{x}} = |w_{\mathbf{x}}|\,\mathrm{e}^{\,j(m-1)\phi_{\mathbf{x}}}$ is a circular complex random variable with zero mean and variance $|w_{\mathbf{x}}|^2$. The associated array factor has zero mean and variance

$$\begin{aligned}
\sigma^2 &= \text{Expectation}\left\{\left|\sum_{\mathbf{x}\in\left\{\substack{\text{element}\\\text{positions}}\right\}} w_{\mathbf{x}}\,\mathrm{e}^{\,j\mathbf{k}\cdot\mathbf{x}}\right|^2\right\} \\
&= \sum_{\mathbf{x},\mathbf{y}\in\left\{\substack{\text{element}\\\text{positions}}\right\}} \text{Expectation}\left(w_{\mathbf{x}}w_{\mathbf{y}}^*\right)\mathrm{e}^{\,j\mathbf{k}\cdot(\mathbf{x}-\mathbf{y})} \\
&= \sum_{\mathbf{x}\in\left\{\substack{\text{element}\\\text{positions}}\right\}} |w_{\mathbf{x}}|^2.
\end{aligned}$$

This is just the energy in the system's conventional taper or array factor and is not a function of $\mathbf{k}$. In fact it's exactly the same as the ratio by which the array as a whole magnifies the spectral height of white noise at each element, assuming all elements have identical preamps and therefore identical white-noise levels and that no noise is introduced elsewhere. As a result of this parallel, for an array of N elements the average factor by which the power in an out-of-band nonlinear term is scaled by this random-phase scheme is

$$\frac{1}{N \times \langle\text{taper efficiency}\rangle}.$$

In this discussion the weights have been assumed random in an ensemble sense. They may or may not also vary with time. If the weights are random but fixed in time, the array factor governing the response to harmonic and harmonic-IMD terms is also random but fixed in time, and while its variance is known, most likely nicely small, and independent of $\mathbf{k}$, the actual array-factor value will indeed vary with $\mathbf{k}$ and may for some particular $\mathbf{k}$ values happen to "peak up" significantly. A random variable with a small variance is not prohibited from being large, after all. It just isn't likely to be.

Re-choosing the random phases from time to time, perhaps on every dwell, would make a peaked-up nonlinear term unlikely to be so for more than one dwell. But this very modest benefit would come at the probably unacceptable cost of making the analog phase shifters controllable.

5.4 Random Delays

With Rabideau's method, providing constant analog and digital phase shifts are expensive and trivial, respectively. An alternative (brought to this author from R. Duncan via D. Scholnik, both of NRL) that makes the analog and digital adjustments respectively trivial and somewhat involved but tolerably so is to use analog delays compensated in-band by digital delay filters.

A (very) preliminary analysis goes like this. Let us decompose signal frequency ω and its mth harmonic modulo sampling rate ω_s as

$$\begin{aligned} \omega &= M\omega_s + \omega_1 \\ m\omega &= (M + \Delta M)\omega_s + \omega_m. \end{aligned}$$

Then an analog factor of $\mathrm{e}^{-j\omega\tau}$ becomes $\mathrm{e}^{-jm\omega\tau} = \mathrm{e}^{-j((M+\Delta M)\omega_s+\omega_m)\tau}$ in the nonlinearity. But the post-nonlinearity compensation sees it only after aliasing and effectively assumes $\Delta M = 0$, compensating with $\mathrm{e}^{j(M\omega_s+\omega_m)\tau}$, give or take causality shimming, for a net phase factor of $\mathrm{e}^{-j\Delta M\omega_s\tau}$. The desired failure to compensate appears whenever the nonlinear term passes through a different digital-filter passband in Fig. 1, which in fact happens for all harmonic and harmonic-IMD terms. Care must be taken to make this net phase factor as close to uniformly distributed on the circle and uncorrelated element to element as possible. The latter certainly requires randomization of τ across elements.

6. CONCLUSIONS

Source terms suppressed by analog-filter stopbands will generate weaker nonlinear terms. This is the first of two classic ways to prevent trouble with ADC nonlinearities.

High-order nonlinearities of all types benefit from input attenuation prior to the nonlinearity. This the second of two classic ways.

In addition, many harmonic and harmonic-IMD terms will be subject to the full suppression of the stopbands of the digital receiver's digital filters. The proportion of harmonic and harmonic-IMD terms that fall into those stopbands is the ratio of final signal-band width (after all sampling-rate reductions, both pre-tuning and post-tuning) to initial sampling rate. In reasonable system configurations, minimizing this rate by maximizing the ADC sample rate will eliminate most out-of-band nonlinear terms. Those that remain will be shifted in frequency by aliasing, and as a result many will fall outside Doppler-filtering boundaries.

Harmonic and many harmonic-IMD terms will not compress well, and neither will in-band IMD created from one radar-signal term and one CW interferer. So a high pulse-compression ratio, i.e. a high time-bandwidth product, will contribute more rejection.

Rabideau's random phase shifts will help significantly—improvement on the order of the array noise gain—with harmonic and harmonic-IMD terms. It is of no help with in-band IMD. None of the other phase-shift approaches suggested thus far look helpful in any but the most special of special cases.

The random time delays of Duncan et al. may be a less expensive but still nontrivial alternative to Rabideau's approach. At best it offers the same benefits. It may be harder to set up with all the desired features, however. Further analysis would be required.

At this time no viable mitigation strategy for in-band IMD created from two radar-signal terms is available. This appears to be an unavoidable vulnerability. Amplitude-modulated waveforms can only make matters worse, not better.

ACKNOWLEDGMENTS

This work was supported by the FlexDAR component of the InTop program of the Office of Naval Research.

REFERENCES

1. K. C. Lauritzen, "Correlation of signals, noise, and harmonics in parallel analog-to-digital converter arrays," Ph.D. dissertation, University of Maryland, College Park, 2009. Obtain at http://hdl.handle.net/1903/9608

2. W. Yu, S. Sen, and B. Leung, "Distortion analysis of MOS track-and-hold sampling mixers using time-varying volterra series," *IEEE Trans. Circuits Syst. II, Analog Digit. Signal Process.*, **46**(2), 101–113, Feb. 1999.

3. L. Howard, N. Simon, and D. Rabideau, "Mitigation of correlated non-linearities in digital phased arrays using channel-dependent phase shifts," in *IEEE MTT-S Int'l Microwave Symp.*, June 2003, 1525–1528 (vol. 3).

4. D. Rabideau, "Hybrid mitigation of distortion in digital arrays," in *IEEE Int'l Radar Conf.*, May 2005, 236–241.

5. A. Gupta and J. Buckwalter, "Spur Free Dynamic Range Prediction for Phased Array Receivers," *IEEE Trans. Antennas Propag.*, 2012.

6. J. O. Coleman, "Wideband IQ downconversion: Part I—Sample rates, IF frequencies, and basic architectures," Naval Research Laboratory, Washington DC, USA, Memo Report NRL/MR/5320--13-9466, estimated pub. date mid-2013.

7. ——, "Signals and systems II," *IEEE Potentials*, **29**(1,2,3,4,5,6), 2010, in six parts.

8. ——, "Planar arrays on lattices and their FFT steering, a primer," Naval Research Laboratory, Washington DC, USA, Formal Report NRL/FR/5320--11-10,207, Apr. 29, 2011. Obtain at http://www.dtic.mil/docs/citations/ADA544059